Title

The Contribution of the Circadian Gene Bmal1 to Female Fertility and the Generation of the Preovulatory Luteinizing Hormone Surge

Journal

Journal of the Endocrine Society, 3(4)

ISSN

2472-1972

Authors

Tonsfeldt, Karen J
Schoeller, Erica L
Brusman, Liza E
et al.

Publication Date

2019-04-01

DOI

10.1210/js.2018-00228

Peer reviewed

ISSN 2472-1972

The Contribution of the Circadian Gene *Bmal1* to Female Fertility and the Generation of the Preovulatory Luteinizing Hormone Surge

Karen J. Tonsfeldt,[1] Erica L. Schoeller,[1] Liza E. Brusman,[1] Laura J. Cui,[1] Jinkwon Lee,[1] and Pamela L. Mellon[1]

[1]*Department of Obstetrics, Gynecology, and Reproductive Sciences, Center for Reproductive Science and Medicine, University of California San Diego, La Jolla, California 92093*

ORCiD numbers: 0000-0001-8044-8857 (K. J. Tonsfeldt); 0000-0002-3355-5964 (E. L. Schoeller); 0000-0001-6180-078X (L. J. Cui); 0000-0002-8856-0410 (P. L. Mellon).

In rodents, the preovulatory LH surge is temporally gated, but the timing cue is unknown. Estrogen primes neurons in the anteroventral periventricular nucleus (AVPV) to secrete kisspeptin, which potently activates GnRH neurons to release GnRH, eliciting a surge of LH to induce ovulation. Deletion of the circadian clock gene *Bmal1* results in infertility. Previous studies have found that *Bmal1* knockout (KO) females do not display an LH surge at any time of day. We sought to determine whether neuroendocrine disruption contributes to the absence of the LH surge. Because *Kiss1* expression in the AVPV is critical for regulating ovulation, we hypothesized that this population is disrupted in *Bmal1* KO females. However, we found an appropriate rise in AVPV *Kiss1* and *Fos* mRNA at the time of lights out in ovariectomized estrogen-treated animals, despite the absence of a measureable increase in LH. Furthermore, *Bmal1* KO females have significantly increased LH response to kiss-10 administration, although the LH response to GnRH was unchanged. We then created Kiss1- and GnRH-specific Bmal1 KO mice to examine whether *Bmal1* expression is necessary within either kisspeptin or GnRH neurons. We detected no significant differences in any measured reproductive parameter. Our results indicate that disruption of the hypothalamic regulation of fertility in the *Bmal1* KO females is not dependent on endogenous clocks within either the GnRH or kisspeptin neurons.

Freeform/Key Words: Bmal1, circadian rhythms, GnRH, kisspeptin, LH

Ovulation in mammals is regulated by the hypothalamic–pituitary–gonadal axis. On the day of rodent proestrus, rising estrogen levels prime kisspeptin (Kiss1) neurons in the anteroventral periventricular nucleus (AVPV). Once activated, these neurons release Kiss1 onto GnRH neurons, which prompts the release of a bolus of GnRH. This surge of GnRH stimulates gonadotropes in the pituitary to release LH and FSH in a similar surge, which prompts ovulation. Both estrogen and a circadian signal "gate" the surge to the end of the subjective night [1].

Circadian rhythms function through a complex molecular feedback loop, the components of which are expressed in most cells in the body. In this feedback loop, the transcription factors CLOCK and BMAL1 dimerize and initiate transcription of clock-controlled genes, including

Abbreviations: ARC, arcuate nucleus; AVPV, anteroventral periventricular nucleus; DAPI, 4′,6-diamidino-2-phenylindole; EB, β-estradiol; Kiss1, kisspeptin; KO, knockout; Per2, Period 2; POA, preoptic nucleus; qPCR, quantitative real-time PCR; SCN, suprachiasmatic nucleus; TH, tyrosine hydroxylase; WT, wild-type; ZT, zeitgeber time.

Received 27 July 2018
Accepted 8 February 2019
First Published Online 13 February 2019

the molecular clock components *Cryptochrome* (*Cry1* and *Cry2*) and *Period* (*Per1*, *Per2*, and *Per3*). CRY and PER dimerize and suppress their own transcription in a 24-hour oscillation. *Bmal1* is the only clock component where singular knockout (KO) results in complete behavioral arrythmicity [2]. The master circadian clock, the suprachiasmatic nucleus (SCN), located in the hypothalamus, sends direct vasopressin-containing projections to AVPV Kiss1 neurons [3, 4] and vasoactive intestinal peptide-containing projections to GnRH neurons [5, 6]. Additionally, *Bmal1* and other clock genes have been identified in Kiss1 neurons, GnRH neurons, and pituitary, indicating several sites of potential temporal regulation of the preovulatory surge and fertility [7–9].

In GnRH neurons *in vitro*, disruption of endogenous circadian rhythms affects GnRH release and Kiss1 receptor expression [10, 11]. *Bmal1* has been localized to Kiss1 neurons in both the AVPV and arcuate nucleus (ARC) [7, 12]. *Kiss1* production and *Fos*, an immediate early gene and marker of neuronal activation, are upregulated in the AVPV at the time of the preovulatory LH surge [13], which only occurs in the presence of estrogen and in the late subjective afternoon. Importantly, this upregulation persists in constant darkness, indicating a circadian component to this regulation, which may arise from SCN projections to the AVPV or endogenous clocks within AVPV Kiss1 neurons. From this work, it has been hypothesized that the endogenous clocks within GnRH or Kiss1 neurons provide temporal gating of the preovulatory surge [3].

Bmal1 KO males and females are infertile [2, 14]. In females, the infertility is due in part to a defect in progesterone synthesis in the ovary, resulting in implantation failure [14]. However, the somatic *Bmal1* KO also confers hypothalamic disruptions: steroidogenic cell–specific *Bmal1* KO ovaries are capable of producing offspring when transplanted into a wild-type (WT) animal, indicating that the inability to sustain pregnancy in the somatic *Bmal1* KOs is not strictly ovarian [15]. Furthermore, gonadotrope-specific *Bmal1* KO mice have no reproductive deficits, indicating that *Bmal1* in the pituitary is not regulating the reproductive phenotype of the somatic *Bmal1* KO [16]. Of considerable interest is the finding that the *Bmal1* KO female ovulates (although infrequently), but it shows no detectable LH surge as measured by LH sampling every 3 hours through proestrus and estrus [16]. A similar phenotype has been described in the *Clock/Clock* mutant mouse, which possesses a dominant-negative form of *Clock* that arrests the molecular clock [17]. These findings indicate differential regulation of the hypothalamic–pituitary–gonadal axis in these animals, although whether this disruption arises from loss of clock genes at the level of the SCN, GnRH, or Kiss1 neurons is unknown. To address this question, we sought to determine whether an LH surge could be induced in *Bmal1* KO females at the appropriate time, and whether hypothalamic–pituitary–gonadal axis function was intact in these mice. We also sought to determine whether *Bmal1* within either GnRH or Kiss1 neurons is responsible for the LH surge defect in the somatic *Bmal1* KO females.

1. Materials and Methods

A. Animals

Bmal1 floxed mice [18] were obtained from The Jackson Laboratory (Bar Harbor, ME) and used to generate the global and conditional *Bmal1* KO lines [19]. Global *Bmal1* KO mice were obtained by crossing a *Bmal1* floxed mouse with a ZP3-Cre mouse [20], as described and validated in Schoeller *et al.* [21]. *Bmal1* KO mice were maintained through heterozygous matings, with WT littermates serving as controls.

The GnRH-Bmal1$^{-/-}$ mouse was created by crossing a GnRH-Cre mouse (from Dr. Andrew Wolfe, Johns Hopkins University School of Medicine, Baltimore, MD) [22, 23] with the *Bmal1* floxed mouse. The Kiss-Bmal1$^{-/-}$ mouse was created by crossing a Kiss-Cre mouse (from Dr. Carol Elias, University of Michigan, Ann Arbor, MI) [24, 25] with the *Bmal1* floxed mouse. The Alb-Bmal1$^{-/-}$ mouse was created by crossing an Albumin-Cre mouse from The Jackson Laboratory [26, 27] with the *Bmal1* floxed mouse. Resulting offspring homozygous for the

Bmal1 flox allele and heterozygous for Cre were used for experiments; homozygous flox, cre-negative littermates were used as controls ($Bmal1^{fl/fl}$). All mice were genotyped using PCR with tail DNA. Genotyping of all lines, as well as recombination evaluation, was performed using the following genotyping primers: Bmal1F1, 5′-CTGGAAGTAACTTTATCAAACTG-3′; Bmal1F2, 5′-CTCCTAACTTGGTTTTTGTCT-3′; Bmal1R, 5′-GACCAACTTGCTAACAATTA-3′; CreF, 5′-GCATTACCGGTCGTAGCAACGAGTG-3′; CreR, 5′-GAACGCTAGAGCCTGT-TTTGCACGTTC-3′. Mice with germline recombination were excluded from analysis. Mice were housed under a 12-hour light/12-hour dark cycle (lights on at 0600 hours) with *ad libitum* access to food and water except where noted. All procedures were approved by the University of California San Diego Institutional Animal Care and Use Committee.

B. GnRH and Kisspeptin Challenges

For GnRH and kisspeptin challenges, a baseline tail vein blood sample was collected. After IP injection of GnRH (catalog no. L7134; Sigma-Aldrich, St. Louis, MO) or kiss-10 (catalog no. 4243; Tocris Bioscience, Bristol, UK), tail vein blood samples (10 μL) were collected after the indicated time. GnRH was injected at 1 μg/kg. For the single kiss-10 challenge and time course, 30 nmol was administered (~2 mg/kg). For the kiss-10 dose-response curve, kisspeptin was tested at 0.01 to 3 mg/kg. Animals were allowed to recover for at least 1 week between doses. For the two sequential kiss-10 challenges, a dose of 2 mg/kg was used. All challenges were performed between zeitgeber time (ZT)6 and ZT8 in diestrus animals. For the dose response, kiss-10 doses were given in a random order across groups. Blood was allowed to clot for 90 minutes and then centrifuged at 2000 × *g* for 15 minutes. Serum was collected and stored at −20°C until LH measurement. Samples were run in singlet on a Milliplex analyzer (MPTMAG-49K; MilliporeSigma, Burlington, MA) using a Luminex Magpix (LH: lower detection limit, 4.8 pg/mL; intraassay coefficient of variation, 15.2%; interassay coefficient of variation, 4.7%).

C. Fertility Assays

Estrous cycling was performed by morning vaginal lavage for at least 21 consecutive days. Vaginal swabs were collected, dried, stained with methylene blue, and scored for the presence of leukocytic cells, small nucleated cells, large nucleated cells, and anucleated cells [28]. Fertility and fecundity were measured following male/female pairings for 100 days. Males used were nonrelated WT mice. Time to first litter, total number of litters, and average litter size at weaning were recorded for all pairs.

D. Pubertal Onset Measurement

In females, pubertal onset was measured by daily inspection for the presence of a vaginal opening as determined by visual assessment of the vulva [29]. Postnatal day and body weights were measured on the day of pubertal onset, as body weight is known to influence the onset of puberty [30].

E. LH Surge Paradigm

The LH surge was induced using an injection paradigm described in Bosch *et al.* [31]. Briefly, animals underwent bilateral ovariectomy. Five days following the procedure, animals were given a subcutaneous injection of 0.25 μg of β-estradiol (EB; catalog no. E8875; Sigma-Aldrich) in 100 μL of sesame oil (catalog no. S3547; Sigma-Aldrich) at ZT10. On the following day, the animals were given a subcutaneous injection of 1.5 μg of EB in sesame oil (100 μL) at ZT10. On the following day, 7 days after ovariectomy, the animals were euthanized at ZT4 (1000 hours) or ZT12 (lights off; 1800 hours) and blood was collected for LH measurement.

F. Measurement of mRNA Expression in Tissue Samples

mRNA was measured from fresh-frozen pituitary or brain. Brains and pituitaries were removed following decapitation and placed immediately on dry ice. The brains and pituitaries were stored at −80°C until micropunch or RNA isolation. All micropunches were 2 mm in diameter and punched from 200-μm-thick brain sections sliced on a cryostat (Leica Biosystems, Wetzlar, Germany) and were guided by a mouse brain atlas [32].

F-1. AVPV

Collection began when the anterior commissure connected (bregma 0.26 mm) and ended at the start of the SCN, which was inferred by the flattening of the optic nerve and the disappearance of the anterior commissure (bregma −0.10 mm). One punch was taken per slice (two to three slices per animal). The punch was oriented up so that it contained the region ventral to the anterior commissure, right along the midline.

F-2. ARC

Collection began with the development of the median eminence at the anterior (bregma −1.58 mm) and ended at the shortening of the third ventricle (bregma −2.18 mm). One punch was taken per slice, and the punch was so that only the ventral portion of the slice was taken, with the apex of the punch approximately halfway down the third ventricle. Three to four slices were taken per animal.

F-3. Preoptic area

Preoptic area (POA) punches were taken from the medial portion of the brain between the anterior commissure bulbs, beginning at the appearance of the lateral ventricles (bregma 1.10 mm) and extending to the bridging of the anterior commissure (bregma 0.38 mm). One punch was taken per slice, two to three slices per animal.

For other studies, whole hypothalami were grossly dissected from the ventral surface of the brain. RNA was extracted using the RNeasy Micro Plus kit (Qiagen, Venlo, Netherlands), 500 ng of total RNA was reverse transcribed using iScript (Bio-Rad Laboratories, Hercules, CA), and the cDNA was stored at −20°C until use in quantitative real-time PCR (qPCR).

To detect gene expression, qPCR was performed on each cDNA sample in triplicate using the Bio-Rad CFX Connect real-time system and the SYBR Green Master Mix (Bio-Rad Laboratories). Standard curves were generated for each product using a dilution series for each primer set to verify 100% ± 5% efficiency, and a single product was verified using melt curve analysis. Products were sequenced for confirmation (Eton Biosciences, San Diego, CA). Data were analyzed using *H2afz* and *Ppia* as housekeeping genes using the $2^{-\Delta\Delta CT}$ quantification method. Primers are shown in Table 1. All findings are reported as fold change relative to the indicated control.

G. Constant Darkness Conditions

Mice were anesthetized with isoflurane and implanted with sterile radio telemeters (Mini Mitter, Bend, OR) and allowed to recover for 1 week. Following recovery, mice were individually housed and acclimated to chambers in 12-hour light/12-hour dark conditions for 4 weeks and then changed to constant darkness conditions for 6 weeks. Ovaries were collected at the time of euthanization for histology. Telemetry data were analyzed using ClockLab (Actimetrics, Wilmette, IL).

H. Ovarian Histology

Ovaries were collected from mice upon euthanization and immediately placed in tissue fixation solution (60% ethanol, 30% formaldehyde, 10% glacial acetic acid) for 24 hours. The

Table 1. Primers for qPCR

Gene	Forward (5′→3′)	Reverse (5′→3′)
H2afz	TCACCGCAGAGGTACTTGAG	GATGTGTGGGATGACACCA
Ppia	AAGTTCCAAAGACAGCAGAAAAC	CTCAAATTTCTCTCCGTAGATGG
cFos	GGCAAAGTAGAGCAGCTATCTCCT	TCAGCTCCCTCCTCCGATTC
Kiss1	TGCTGCTTCTCCTCTGT	ACCGCGATTCCTTTTCC
GnRH	ACACTTGGTTGAGTCTTTCCA	TGGCTTCCTCTTCAATCAGAC
V1a	AGCGCCTACATCCTCTGCTG	AGTAACGCCGTGATCGTGGT
Dynorphin	GTGTGCAGTGAGGATTCAGG	AGTCATCCTTGCCACGGAGC
Kiss1R	GACCATGCAGACAGTTACC	GCAGCACAGTAGGAAAGTGAC
TH	CAGCCCTACCAAGATCAAAC	GTGTACGGGTCAAACTTCA
FSHβ	GCCGTTTCTGCATAAGC	CAATCTTACGGTCTCGTATACC
LHβ	CTGTCAACGCAACTCTGG	ACAGGAGGCAAAGCAGC
GnRH-R	GCCCCTTGCTGTACAAAGC	CCGTCTGCTAGGTAGATCATCC

Abbreviation: TH, tyrosine hydroxylase.

solution was changed to 70% ethanol the following day and replaced with fresh 70% ethanol after 24 hours. Tissue was dehydrated and processed for paraffin embedding. The ovaries were sectioned using a microtome at 20 μm, with three to four sections per slide, and dried overnight at 37°C. A hematoxylin and eosin stain (Sigma-Aldrich) was used to distinguish ovarian morphology. Corpora lutea and Graafian follicles were counted on every fifth section for each sectioned ovary. The section with the greatest number of corpora lutea or Graafian follicles was used as the representative number for that animal.

I. Immunofluorescence

Brains were dissected at the time of euthanization for the LH surge (lights off, ZT12). Brains were fixed in a solution made of 30% formaldehyde, 60% ethanol, and 10% glacial acetic acid and placed on a shaker. The following 2 days, brains were transferred to fresh 70% ethanol. Brains were paraffin embedded and cut in 10-μm sections on a microtome. Slides were deparrafinized using Histo-Clear (National Diagnostics, Atlanta, GA) and underwent antigen retrieval in Citra buffer (BioGenex, Fremont, CA) in a 2100 Retriever (Aptum Biologics, Southampton, UK). Slides were blocked in Bloxall (Vector Laboratories, Burlingame, CA), followed by an avidin and protein block (Vector Laboratories). Slides were incubated overnight in 1:5000 guinea pig anti-Bmal1 (catalog no. AB2204; EMD Millipore, Temecula, CA) [33] and 1:2000 rabbit anti-GnRH (catalog no. 20075; ImmunoStar, Hudson, WI) [35]. To visualize BMAL1, slides were incubated in 1:300 biotin anti–guinea pig (catalog no. BA-7000; Vector Laboratories) [36] for 1 hour, an ABC reagent (Vector Laboratories) for 30 minutes, a biotinylated tyramide (PerkinElmer, Waltham, MA) for 10 minutes, and then 1:200 streptavidin DyLight 488 (Invitrogen, Rockford, IL) for 30 minutes. Between steps, slides underwent three to four washes in PBS. All antibody incubations occurred in PBS with 2% Tween 20 (Sigma-Aldrich) and 5% goat serum (Vector Laboratories). To visualize GnRH, slides were then incubated with 1:100 goat anti-rabbit Alexa Fluor 594 (catalog no. A11012; Life Technologies, Eugene, OR) [37] for 30 minutes. Slides were coverslipped using ProLong anti-fade reagent with 4′,6-diamidino-2-phenylindole (DAPI; Cell Signaling Technology, Danvers, MA).

J. Fluorescent Imaging and Colocalization Analysis

All fluorescent images were collected at the University of California San Diego Nikon Imaging Center with a Nikon Eclipse Ti2 equipped with Plan Apo ×20 0.75 numerical aperture or ×40 S Fluor 0.9 numerical aperture objectives. Fluorescence was excited using the Aura II light engine (Lumencor, Beaverton, OR) with 395, 470, or 555 light-emitting diodes. The

images were collected using a Nikon DS-Qi2 camera and NIS Elements 5.10 software. Three independent observers that were blinded to conditions analyzed for colocalization. Images were uploaded to an OMERO server and analyzed using the Fiji distribution of ImageJ [38]. Figures were created using OMERO.webclient [39].

K. Statistical Analysis

T-tests and one- and two-way ANOVA were performed using Prism 6 (GraphPad Software, San Diego, CA) with $P \leq 0.05$ indicating significance. Significant effects were followed with a Sidak *post hoc* test ($P < 0.05$).

2. Results

A. Bmal1 *KO Females Do Not Show an Inducible LH Surge at Lights Out, But They Do Show Time- and Estrogen-Dependent Regulation of AVPV Kiss1 and* Fos

To determine the ability of *Bmal1* KO females to respond to an induced LH surge paradigm, mice were ovariectomized and estrogen treated according to Bosch *et al.* [31]. In this paradigm, mice are allowed to recover from ovariectomy for 4 days, followed by a low-dose (0.5 μg) and high-dose (1.5 μg) injection of EB at ZT4 on recovery days 5 and 6, respectively. On day 7, mice were killed at ZT4 or ZT12 and blood was measured for LH. At ZT4, basal LH levels were measured for WT (1.59 ± 0.20 ng/mL LH, n = 5) and *Bmal1* KO (1.04 ± 0.26 ng/mL LH, n = 5) (Fig. 1A). At ZT12, WT mice show an expected increase in LH (7 of 10 mice had LH values >2.0 ng/mL, which was defined as an LH surge with our LH assay; 4.90 ± 1.35 ng/mL), which was significantly higher than LH levels in the *Bmal1* KO females (8 of 8 mice <2.0 ng/mL LH; 0.82 ± 0.05 ng/mL). These findings are consistent with previously reported data from *Bmal1* KO mice in an endogenous surge model [16].

Because time- and estrogen-dependent regulation of Kiss1 in the AVPV is thought to contribute to the LH surge, we examined mRNA expression of *Kiss1* and *Fos,* an immediate early gene used as a marker of neuronal activation, from AVPV micropunches taken from WT and *Bmal1* KO females from the experiment described above. We found that although both WT and *Bmal1* KO females had a significant increase in *Kiss1* mRNA in the afternoon time points, there was no difference between the groups, indicating a normal time- and estrogen-responsive *Kiss1* increase in *Bmal1* KO females (Fig. 1B). Similarly, *Fos* was significantly upregulated at the time of the LH surge, but there was no significant difference between WT and *Bmal1* KO levels at either time point (Fig. 1C).

B. Bmal1 *KO Females Have Increased Responsiveness to Kisspeptin*

Because AVPV *Kiss1* production and estrogen responsiveness is intact in *Bmal1* KO females, and this region is activated during the time of the LH surge, we next wanted to determine whether LH responsiveness to hypothalamic peptide stimulation was altered. All experiments were performed around ZT4 in diestrous females. We found that 1 μg/kg IP GnRH significantly increased LH after 10 minutes in both WT and *Bmal1* KO mice, but there was no significant difference between WT and *Bmal1* KO in the LH values, indicating normal pituitary responsiveness to GnRH (Fig. 2A). Next, we administered 30 nmol of kiss-10 IP and measured subsequent serum LH responses after 10 minutes. We saw a significant increase in serum LH in *Bmal1* KO females compared with WT mice (Fig. 2B).

To determine whether the increased responsiveness to kisspeptin in *Bmal1* KO females was due to a difference in kisspeptin metabolism, we performed a time course and examined the LH response to 30 nmol of kisspeptin after 5, 10, 15, 20, 30, and 45 minutes (Fig. 3A). *Bmal1* KO females had an increased LH response to kiss-10, as well as an increased area under the curve (Fig. 3A and 3B).

Next, we examined the dose-response relationship between kisspeptin treatment and LH response in *Bmal1* KO and WT females. Diestrous mice were administered 0.01 to 3.0 mg/kg kiss-10, and serum LH was measured after 10 minutes (for comparison, the 30-nmol dose

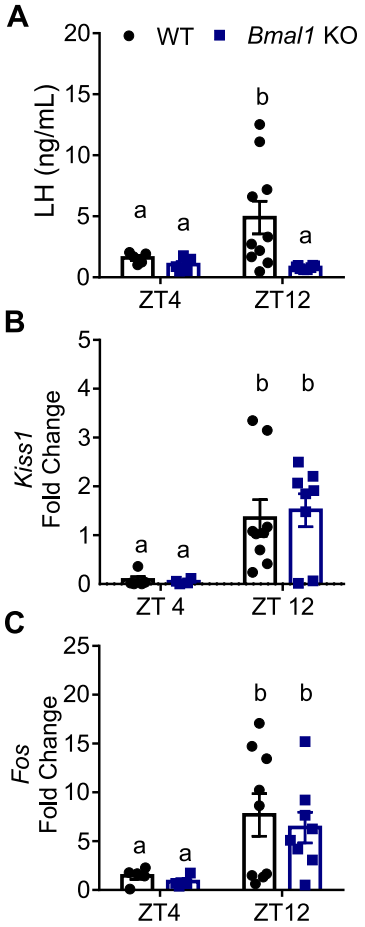

Figure 1. *Bmal1* KO females do not display an LH surge at lights out, despite increased AVPV *Kiss1* and *Fos* mRNA. (A) LH values at ZT4 and ZT12 (lights off) in an induced surge model (n = 5 to 10; two-way ANOVA, effect of genotype; $F_{1,24} = 4.99$, $P = 0.035$); Sidak *post hoc* multiple comparisons test). (B) *Kiss1* mRNA fold change relative to WT ZT12 from AVPV micropunches (n = 4 to 9; two-way ANOVA, effect of time; $F_{1,22} = 14.44$, $P = 0.0010$). (C) *Fos* mRNA fold change relative to WT ZT4 from AVPV micropunches (n = 4 to 9; two-way ANOVA, effect of time; $F_{1,22} = 9.147$, $P = 0.0062$). Different letters indicate significantly different groups ($P < 0.05$).

used in the time course is ~2 mg/kg for a 20 g mouse). Post–kiss-10 LH values were fit to a four-parameter logistic curve, where the model favored different curves for the *Bmal1* KO vs WT response (comparison of fits, $P < 0.016$; Fig. 3C). There was no significant difference in the EC50 or Hill slope, but the maximum was significantly greater in the *Bmal1* KO (4.18 ± 0.61 ng of LH) vs WT mice (2.11 ± 0.2 ng of LH; $P < 0.018$, *t* test).

To determine whether the increase response to kiss-10 may be due to lower kisspeptin levels in the *Bmal1* KO animals, we performed two kiss-10 challenges 1 hour apart to "prime" the hypothalamus. Challenges 1 and 2 occurred as described above: prechallenge tail blood was sampled, animals were administered 2 mg/kg kiss-10, and postchallenge blood was collected 10 minutes later. One hour after the first trial, we performed an identical challenge on the same mice. We found that the LH response in *Bmal1* KO females in the second challenge was significantly higher than in the first challenge (Fig. 3D).

Bmal1 in the liver has been implicated in drug metabolism [40–42]; to further confirm that the heightened response to kisspeptin was not due to a metabolic effect, we also compared kisspeptin responsiveness in the liver-specific *Bmal1* KO, Albumin-Cre × $Bmal1^{flox/flox}$ (Alb-$Bmal1^{-/-}$) mice. There was no difference in LH response to kiss-10 in the Alb-$Bmal1^{-/-}$ females compared with females (Fig. 3E and 3F), supporting hypothalamic or pituitary sensitivity to kisspeptin in the *Bmal1* KO mice.

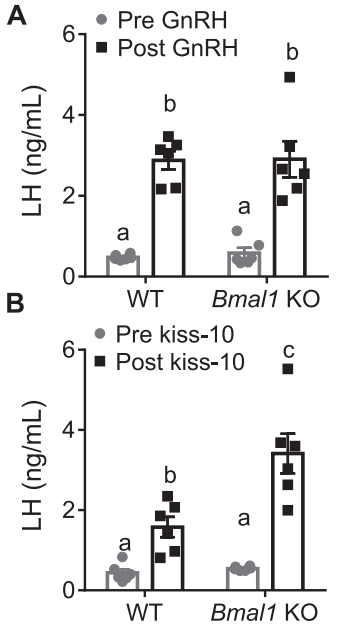

Figure 2. *Bmal1* KO females have normal LH response to GnRH, but heightened LH response to kisspeptin. (A) LH values before and after exposure to 1 μg/kg GnRH (n = 6; two-way ANOVA, effect of time; $F_{1,10} = 88.88$, $P < 0.0001$; Sidak multiple comparisons test). (B) LH values before and after exposure to 30 nmol of kiss-10 (n = 6; two-way ANOVA significant for time and genotype interaction; $F_{1,10} = 8.4$, $P = 0.0159$; Sidak multiple comparisons test). Different letters indicate significantly different groups ($P < 0.05$).

C. Bmal1 *KO Females Have Normal Hypothalamic Gene Expression*

We next evaluated mRNA expression in the ARC, AVPV, POA, and pituitary between *Bmal1* KO and WT females. We hypothesized that *Bmal1* KO females may have an increase in kisspeptin responsiveness due to expression differences in *Dynorphin*, which modulates kisspeptin release, or *Kiss1R*, the kisspeptin receptor, in the ARC or pituitary. We found no significant difference between WT and *Bmal1* KO females in the expression of either gene from ARC micropunches (Fig. 4A). Alternatively, the lack of an LH surge in the *Bmal1* KO mice may be due to an inability to process signals from the SCN. We then examined AVPV expression of V1a, the vasopressin receptor that is proposed to mediate vasopressin-containing signals from the SCN, and tyrosine hydroxylase (TH), which is commonly coexpressed with AVPV Kiss1 neurons and was used to indicate punch quality (Fig. 4B). We found no difference in the expression of these genes from AVPV micropunches between WT and *Bmal1* KO females. We also examined *GnRH* and *Kiss1R* receptor expression from POA micropunches, where we again found no difference in mRNA expression between WT and *Bmal1* KO females (Fig. 4C). Finally, because kisspeptin has been shown to induce LH release from pituitary explants from rats [43], we examined the pituitary for differences in *FSHβ* and *LHβ*, the GnRH receptor (*GnRH-R*), and *Kiss1R* (Fig. 4D). Again, we found no significant differences between WT and *Bmal1* KO animals. These results indicate that the differential response to kisspeptin seen in the *Bmal1* KO females does not appear to be due to the expression of known hypothalamic genes that would regulate basal kisspeptin release, LH or FSH production, or kisspeptin or GnRH responsiveness.

D. Conditional KO of Bmal1 *in GnRH or* Kiss1 *Neurons Has No Effect on Female Fertility*

To determine whether the lack of the LH surge in *Bmal1* KO females could be due to the loss of *Bmal1* in either GnRH or Kiss1 neurons, we created two mouse lines to delete *Bmal1* in these populations: a GnRH-Bmal1$^{-/-}$ mouse, in which GnRH-cre was crossed with Bmal1$^{flox/flox}$

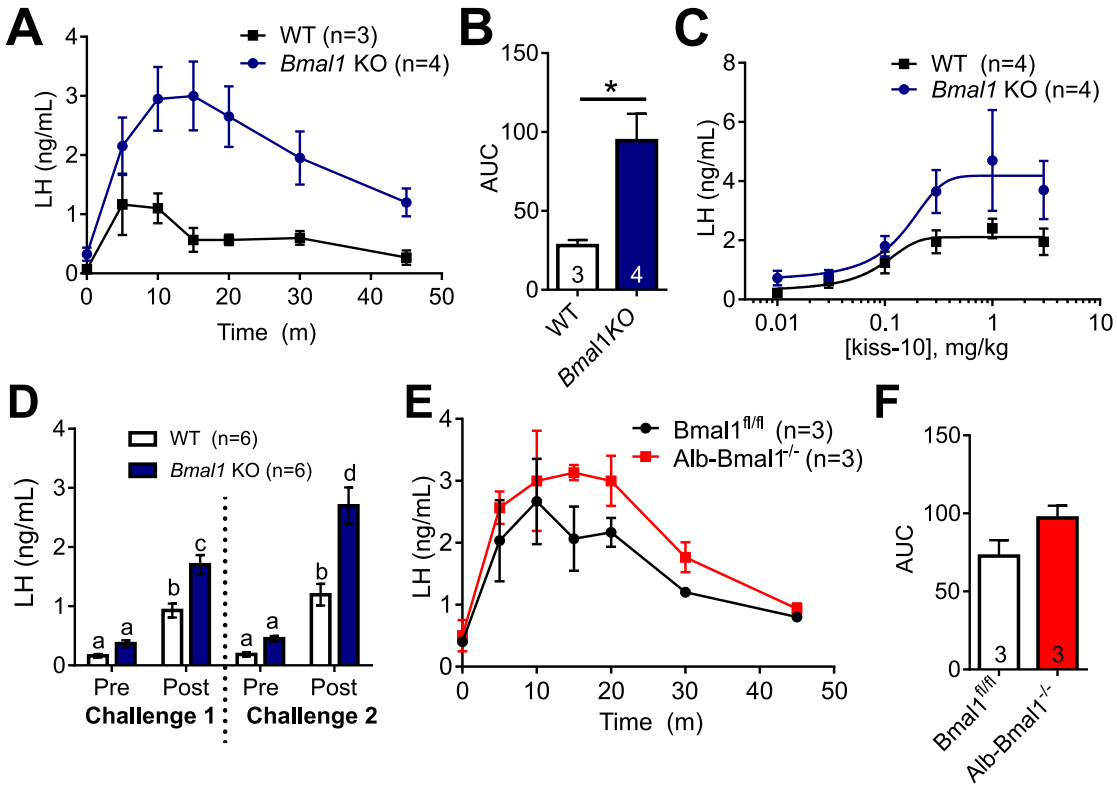

Figure 3. *Bmal1* KO females have prolonged and heightened LH response to kisspeptin, which is not due to loss of *Bmal1* in the liver. (A) LH values following 30 nmol of kiss-10 administration in WT and *Bmal1* KO females (n = 3 to 4; two-way ANOVA, significant for time and genotype interaction; $F_{6,30} = 3.35$, $P = 0.012$). (B) Area under the curve (AUC) of LH response during 45 min (n = 3 to 4; $P = 0.022$; unpaired t test). (C) LH values 10 min after kiss-10 administration (0.01 mg/kg to 3 mg/kg) in WT vs *Bmal1* KO females fit with a four-parameter logistical curve (n = 4; comparison of fits, $P = 0.159$). (D) LH values before and 10 min after 2 mg/kg kiss-10 (challenge 1), and then from a second challenge 1 h later (challenge 2) (n = 6, two-way ANOVA, significant effect of time and genotype; $F_{3,40} = 8.168$, $P = 0.0001$; Sidak multiple comparisons test). (E) LH values following 30 nmol of kiss-10 in $Bmal1^{fl/fl}$ and Albumin-$Bmal1^{-/-}$ females (n = 3; two-way ANOVA significant for time; $F_{6,24} = 14.26$, $P < 0.0001$). (F) AUC of LH response during 45 min (n = 3; $P = 0.13$; unpaired t test).

to knock out *Bmal1* from GnRH neurons, and a Kiss-$Bmal1^{-/-}$ mouse, in which Kiss-cre was crossed with $Bmal1^{flox/flox}$ to knock out *Bmal1* from Kiss1 neurons.

The conditional KO was validated in the GnRH-$Bmal1^{-/-}$ mice using immunofluorescence. In $Bmal1^{fl/fl}$ controls, we found most (73 of 107 neurons; 68%) GnRH neurons coexpressed Bmal1 (Fig. 5A; 24 to 49 cells from three animals). In GnRH-$Bmal1^{-/-}$ animals, we detected colocalization of Bmal1 and GnRH in only 9 of 76 neurons (Fig. 5B; 12%; 11 to 29 cells from four animals). The number of colocalized neurons was significantly reduced between $Bmal1^{fl/fl}$ and GnRH-$Bmal1^{-/-}$ animals, and GnRH colocalization was only detected in one of the four animals examined (Fig. 5C). In the Kiss-$Bmal1^{-/-}$ line, we measured Bmal1 recombination in micropunches from the AVPV, ARC, cortex, thalamus, and cerebellum of $Bmal1^{fl/fl}$ and Kiss-$Bmal1^{-/-}$ animals. Our data show that there was *Bmal1* recombination present in the AVPV and ARC, consistent with an effective conditional KO.

The age (Fig. 6A) and weight (Fig. 6B) of pubertal onset as indicated by vaginal opening was not significantly different between GnRH-$Bmal1^{-/-}$, Kiss-$Bmal1^{-/-}$, and $Bmal1^{fl/fl}$ littermate controls. Daily vaginal cytology revealed no significant differences between the groups in the percentage of time spent in each stage (Fig. 6C) or cycle length (Fig. 6D).

To confirm ovulation histologically, ovaries were collected from GnRH-$Bmal1^{-/-}$, Kiss1-$Bmal1^{-/-}$, and $Bmal1^{fl/fl}$ mice and examined following hematoxylin and eosin staining.

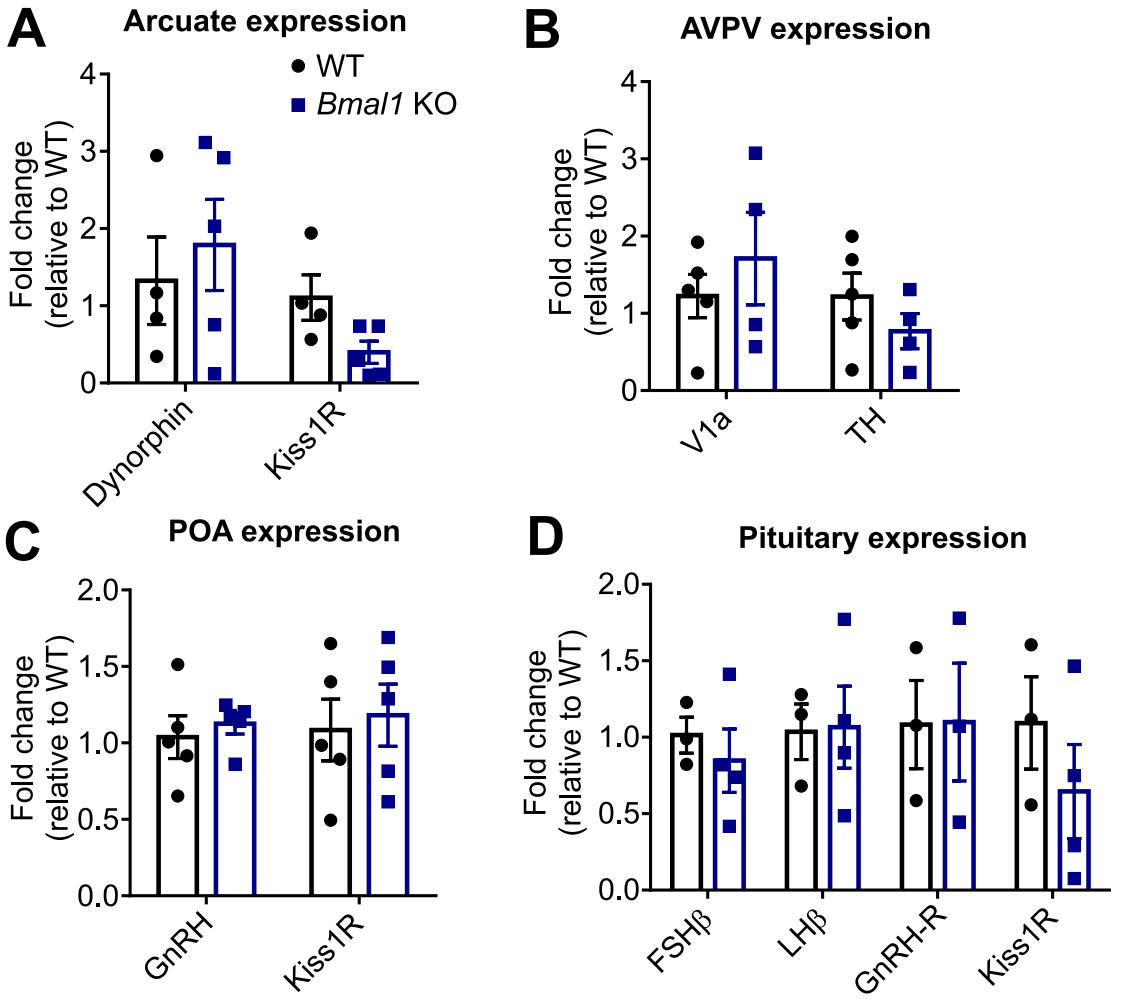

Figure 4. qPCR reveals no significant differences among reproductively relevant hypothalamic and pituitary genes. (A) Arcuate micropunches show no differences between WT and *Bmal1* KO expression of *Dynorphin* or *Kiss1R* (*t* test, n = 4 to 5; Kiss1R, $P = 0.05$). (B) AVPV micropunches show no significant differences between WT and *Bmal1* KO expression of *V1a* or tyrosine hydroxylase (TH; *t* test, n= 4 to 5). (C) POA micropunches show no differences between WT and *Bmal1* KO expression of *Kiss1R* or *GnRH* (*t* test, n = 5). (D) Whole pituitary shows no significant differences among *FSHβ*, *LHβ*, *GnRH-R*, and *Kiss1R* (*t* test, n = 3 to 4; *Kiss1R*, $P > 0.05$).

Graafian follicles and corpora lutea were quantified (Fig. 6E and 6F). Next, we sought to determine whether the entrainment to the light/dark cycle might mask any population-specific KO effects by examining the mice following 6 weeks of constant darkness. GnRH-Bmal1$^{-/-}$ and Kiss1-Bmal1$^{-/-}$ females did not have statistically significant different free-running periods compared with Bmal1$^{fl/fl}$ (Bmal1$^{fl/fl}$, 23.75 ± 0.045, n = 4; GnRH-Bmal1$^{-/-}$, 23.68 ± 0.02, n = 3; Kiss-Bmal1$^{-/-}$, 23.7 ± 0.02, n = 3), indicating no disruption of circadian activity in these mice, as expected. We observed an increase in the number of Graafian follicles in Bmal1$^{fl/fl}$ and Kiss-Bmal1$^{-/-}$ mice in animals in constant darkness and a trend toward an increase in GnRH- Bmal1$^{-/-}$ mice in constant darkness, although this experiment had a small sample size (n = 2) due to a histology error. There were no differences between the groups among respective lighting conditions. We observed no difference in corpora lutea between groups or lighting conditions. Overall, we detected no differences in either structure between the conditional KO mice and Bmal1$^{fl/fl}$ mice, indicating that these mice were still able to ovulate in constant dark conditions.

We did not detect any differences in fecundity between GnRH-Bmal1$^{-/-}$, Kiss-Bmal1$^{-/-}$, or Bmal1$^{fl/fl}$ females. Dams from each genotype were age matched and paired with WT males

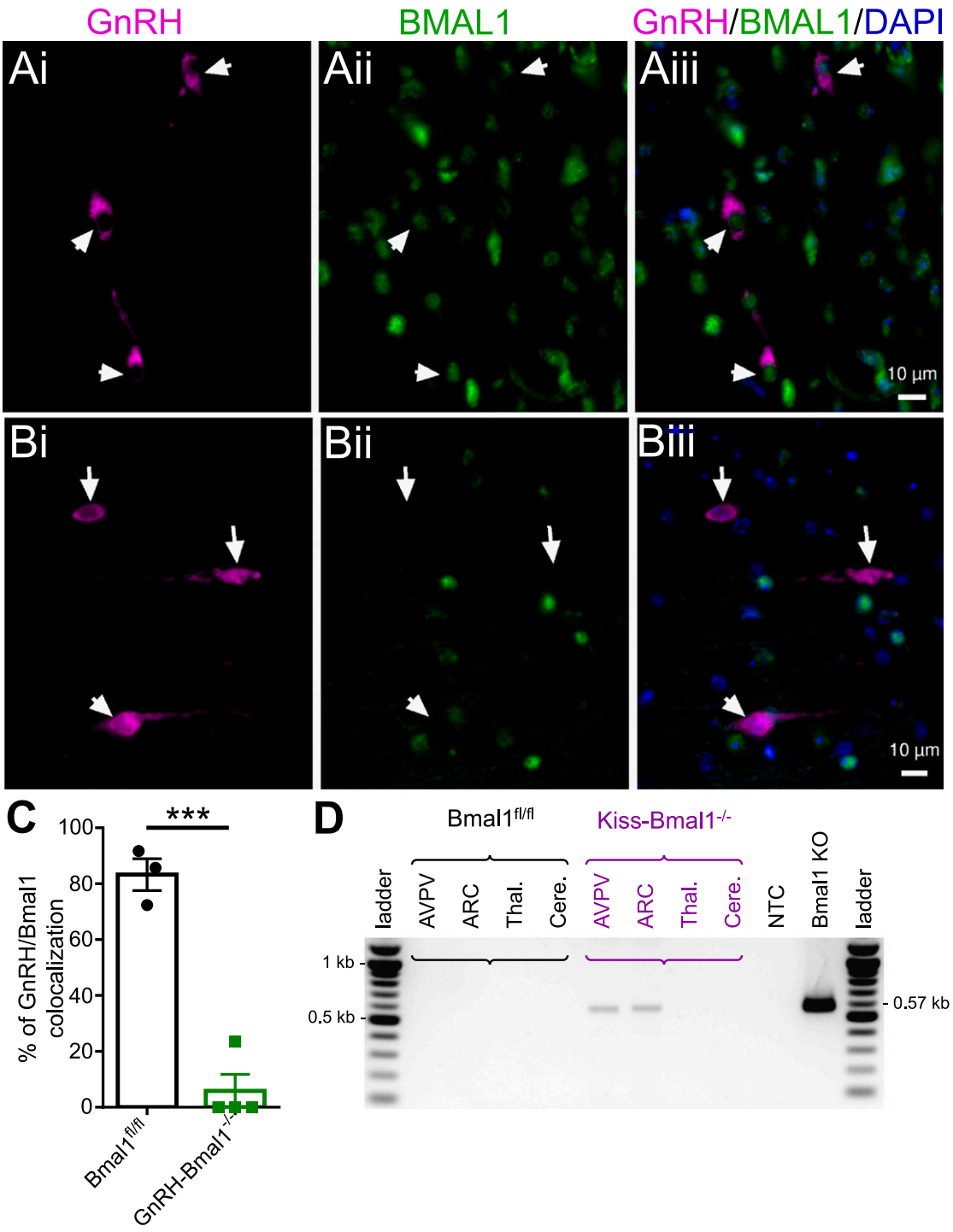

Figure 5. Validation of conditional KO in GnRH-Bmal1$^{-/-}$ and Kiss-Bmal1$^{-/-}$ mice. (Ai) GnRH (magenta), (Aii) BMAL1 (green), and (Aiii) merged image with DAPI (blue) from a Bmal1$^{fl/fl}$ mouse. GnRH neurons are identified by arrowheads in the isolated and merged images. (Bi) GnRH (magenta), (Bii) BMAL1 (green), and (Biii) merged image of with DAPI (blue) from a GnRH-Bmal1$^{-/-}$ mouse. (C) Quantification of the percentage of GnRH and Bmal1 colocalization in Bmal1$^{fl/fl}$ and GnRH-Bmal1$^{-/-}$ mice (*t* test, n = 3 to 4; $P < 0.003$). (D) Representative PCR product from genomic DNA of micropunches showing *Bmal1* recombination in the AVPV and ARC of the Kiss-Bmal1$^{-/-}$ mouse, but not in regions lacking *Kiss1* expression (~0.57-kb band). Recombination in a *Bmal1* KO tail sample is shown as a positive control. ***$P < 0.001$. Cere., cerebellum; NTC, no template control; Thal., thalamus.

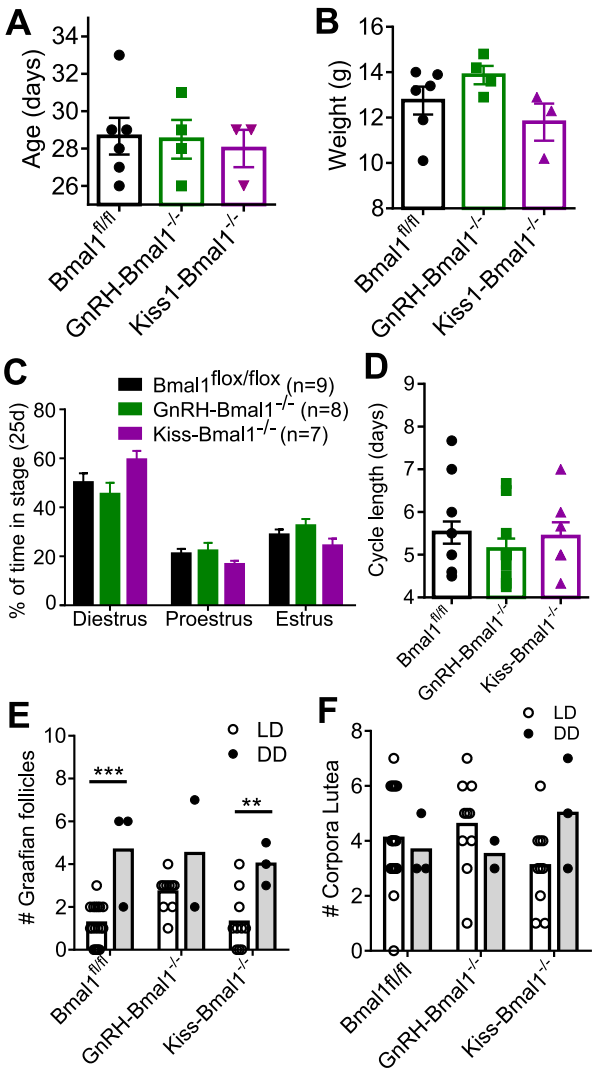

Figure 6. *Bmal1* KO in GnRH or Kiss1 neurons does not affect pubertal onset or estrous cycling. (A) Age (d) and (B) weight (g) of vaginal opening in Bmal1$^{fl/fl}$, GnRH-Bmal1$^{-/-}$, and Kiss-Bmal1$^{-/-}$ female mice (n = 3 to 6; one-way ANOVA not significant). (C) Percentage of time spent in each stage during 25 consecutive days of vaginal cytology (n = 7 to 13, two-way ANOVA significant for effect of stage; $F_{2,51} = 52.15$, $P < 0.0001$). (D) Average cycle length across 25 consecutive days of vaginal cytology (n = 7 to 13; one-way ANOVA not significant). (E) Number of Graafian follicles per section observed in ovaries in light/dark (LD) and constant darkness (DD) conditions (n = 2 to 15, two-way ANOVA significant for effect of lighting; $F_{1,24} = 24.42$, $P < 0.0001$; Sidak *post hoc* multiple comparisons test). (F) Number of corpora lutea observed per section in LD and DD conditions (n = 2 to 15; two-way ANOVA not significant). $^{**}P < 0.01$, $^{***}P < 0.001$.

for 100 days, with additional monitoring for 30 days after the male was removed. During the course of the experiment, there was no difference in the time to first litter (Fig. 7A), number of litters (Fig. 7B), or litter size (Fig. 7C). Overall, these findings reveal no major fertility defects in the GnRH-Bmal1$^{-/-}$ or Kiss-Bmal1$^{-/-}$ mice.

E. GnRH-Bmal1$^{-/-}$ and Kiss-Bmal1$^{-/-}$ Mice Show an Inducible LH Surge and Have Normal Hypothalamic–Pituitary–Gonadal Axis Responsiveness

GnRH-Bmal1$^{-/-}$, Kiss-Bmal1$^{-/-}$, and Bmal1$^{fl/fl}$ littermates were ovariectomized and estrogen treated as described above. We found no difference in serum LH among groups at the

time of lights off, indicating that both the GnRH-Bmal1$^{-/-}$ and Kiss-Bmal1$^{-/-}$ mice are capable of producing an LH surge at the correct time of day (Fig. 8A). These data suggest that the lack of LH surge in the whole-body *Bmal1* KO mouse is not due to loss of *Bmal1* in either GnRH or Kiss1 neurons, or that any few remaining neurons containing *Bmal1* are sufficient to retain enough responsiveness for the surge.

Next, we evaluated the LH response to exogenous GnRH and Kiss1 in gonad-intact, diestrous GnRH-Bmal1$^{-/-}$, Kiss-Bmal1$^{-/-}$, and Bmal1$^{fl/fl}$ mice. GnRH (1 μg/kg IP) significantly increased LH after 10 minutes in all groups, but we detected no significant difference between GnRH-Bmal1$^{-/-}$, Kiss-Bmal1$^{-/-}$, and Bmal1$^{fl/fl}$ females, indicating normal pituitary responsiveness to GnRH (Fig. 8B). Similarly, we found that kisspeptin (30 nmol IP) increased LH in all groups, with no significant differences between the groups (Fig. 8C), and it did not reproduce the increased responsiveness of the *Bmal1* KO mouse. Overall, these findings suggest no major differences in hypothalamic or pituitary responsiveness in the GnRH-Bmal1$^{-/-}$ and Kiss-Bmal1$^{-/-}$ females compared with Bmal1$^{fl/fl}$ females.

3. Discussion

The *Bmal1* KO female fails to produce an LH surge [16], although the mechanism for the loss remains unclear. In this study, we demonstrate that in an induced surge paradigm, *Bmal1* KO females are still capable of appropriate time- and estrogen-dependent *Kiss1* and *Fos* upregulation in the AVPV; however, this is insufficient to generate an LH surge. We demonstrate that the absence of LH release in the presence of increased *Kiss1* mRNA does not arise from a difference in kisspeptin responsiveness; in fact, *Bmal1* KO females show greater LH response to kisspeptin than do WT females. Furthermore, we found no differences in hypothalamic or pituitary gene expression of *FSHβ*, *LHβ*, *GnRH-R*, or *Kiss1R*. We show by Cre-mediated recombination of *Bmal1* in either GnRH or Kiss1 neurons that *Bmal1* in those neuronal populations is not responsible for the infertility, loss of the LH surge, or the increased kisspeptin responsiveness in the *Bmal1* KO mice. These findings suggest that endogenous clocks within these discrete neuronal populations are not necessary for the preovulatory LH surge and fertility, and instead they support the importance of direct SCN projections to Kiss1 and GnRH neurons.

The absence of the LH surge in the *Bmal1* KO female mouse is particularly compelling. Chu *et al.* [16] used intact cycling mice and measured LH every 3 hours from a 24-hour period

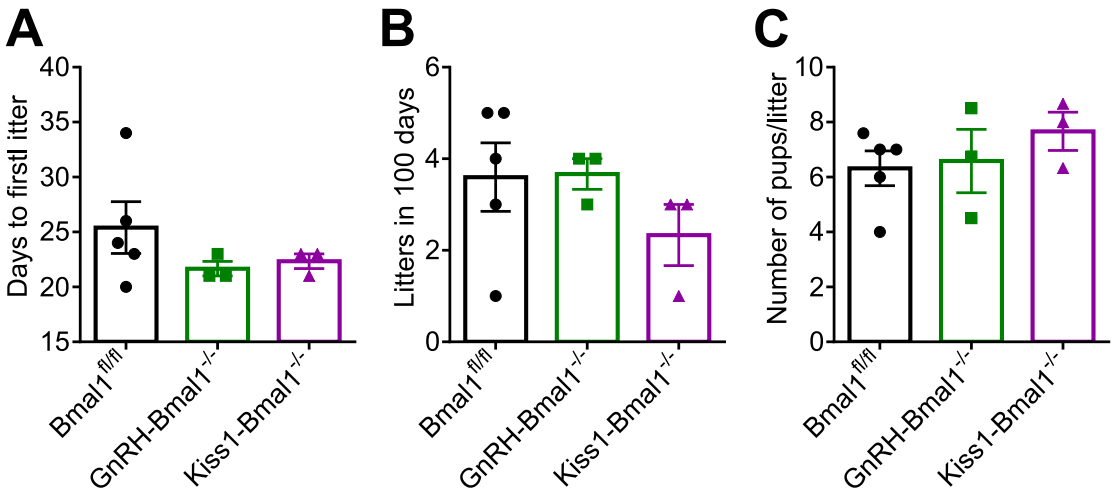

Figure 7. GnRH-Bmal1$^{-/-}$ and Kiss-Bmal1$^{-/-}$ have normal fecundity. (A) Time to first litter as measured by days after pairing (n = 3 to 5; one-way ANOVA not significant). (B) Average number of litters produced in 100 d of pairing, including 25 d of observation following removal of male (n = 3 to 5; one-way ANOVA not significant). (C) Number of pups per litter during recorded period (n = 3 to 5, one-way ANOVA not significant).

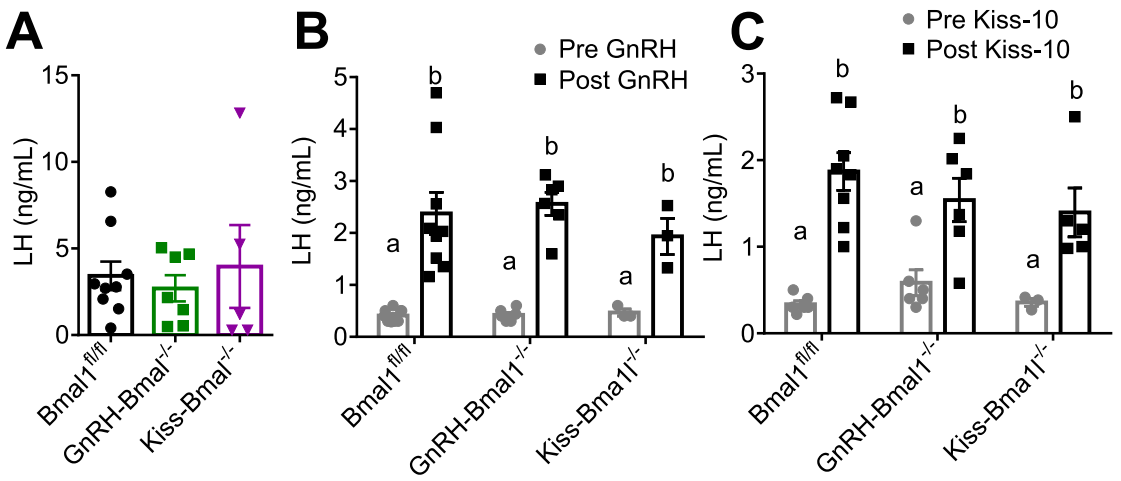

Figure 8. GnRH-Bmal1$^{-/-}$ and Kiss-Bmal1$^{-/-}$ produce an LH surge at lights off and have normal GnRH and kiss-10 LH responsiveness. (A) LH levels at lights off in an induced surge paradigm (for nonsurging example, please see Fig. 1A) (n = 5 to 9, one-way ANOVA not significant). (B) LH levels before and 10 min after 1 μg/kg GnRH administration (n = 3 to 9; two-way ANOVA significant for time; $F_{1,30} = 56.89$, $P < 0.0001$; Sidak multiple comparisons test). (C) LH levels before and 10 min after 30 nmol of kiss-10 administration (n = 3 to 8; two-way ANOVA significant for time; $F_{1,28} = 43.61$, $P < 0.0001$; Sidak multiple comparisons test). Different letters indicate significantly different groups ($P < 0.05$).

beginning early proestrus through estrus. They found no detectable rise in LH in the *Bmal1* KO females, but confirmed ovulation through examination of the oviduct. Although these findings do not conclusively establish that the LH surge did not occur, they do suggest that the dynamics of such a surge are different from those in WT mice. These findings are similar to observations in the *Clock/Clock* mutant mouse, in which an estrogen-induced LH surge model with hourly sampling showed no LH surge as opposed to that in the WT mouse [17]. Our findings support the conclusion that *Bmal1* KO females are unable to generate an LH surge in an estradiol-induced paradigm at lights off. Overall, these data suggest that either dynamics of the LH surge in circadian mutant mice is dramatically different from what is observed in their WT counterparts, or that circadian mutation reveals a noncanonical ovulation mechanism.

Despite the absence of the LH surge, our findings show that *Bmal1* KO females demonstrated increased *Kiss1* and *Fos* mRNA at the time of lights out, suggesting no disruption in the pre-surge AVPV response. Previous work has demonstrated a reliable and repeatable rise in both *Kiss1* and *Fos*, a marker of neuronal activation, at the time of the preovulatory surge [3, 13]. This event persists in constant darkness, indicating that it is controlled by circadian rhythms rather than light [13]. In micropunches from the AVPV, we saw similar increases in both *Kiss1* and *Fos* mRNA in the *Bmal1* KO females as in WT females. Although these findings do not localize *Fos* to the *Kiss1* neurons specifically, these data suggest that the mechanism of Kiss1 neuron activation is intact in the *Bmal1* KO females and may be independent of clock function as a whole.

The absence of an LH surge despite increased AVPV *Kiss1* and *Fos* mRNA and LH responsiveness to kiss-10 injections suggests an interference preventing the canonical surge in the *Bmal1* KO mice. Williams *et al.* [3] showed that in the Syrian hamster, vasopressin administration could drive the increase in AVPV *Kiss1* and *Fos* mRNA and in the morning and afternoon, speculating that a vasopressin signal originating in the SCN drives this phenomenon. In our study, we found that increased *Kiss1* and *Fos* mRNA in the AVPV of *Bmal1* KO mice was not sufficient to produce an LH surge. This finding suggests that the time-dependent rise in AVPV *Kiss1* and *Fos* mRNA may not be a *Bmal1*-dependent process. Coupled with our findings that *Bmal1* KO mice have increased LH responsiveness to kiss-10, these findings may indicate that Kiss1–GnRH connectivity or coordination is altered in

Bmal1 KO mice. However, conditional KO of *Bmal1* in either Kiss1 or GnRH neurons alone is insufficient to reproduce the loss of LH surge or the heightened kisspeptin responsiveness observed in the *Bmal1* KO females.

The greater maximal effect of kisspeptin injections on LH release in the *Bmal1* KO females in the absence of a change in EC50 suggests a greater efficacy of kisspeptin in evoking LH release in *Bmal1* KO females than in WT females. Exogenous kisspeptin administration is thought to stimulate LH release through actions on GnRH neurons [44]. Because we do not see an increase in the LH response to GnRH, it is likely that the effects are occurring upstream of the pituitary at the level of GnRH neurons. A greater bolus of GnRH release in response to kisspeptin would be consistent with our findings from the dose-response curve, although *in vitro* evidence from other groups suggests dampened GnRH release in response to kisspeptin administration in explants from *Bmal1* KOs [45]. However, this may not be the case *in vivo*. We found that *Bmal1* KO mice had an even greater LH response to kisspeptin in a second kiss-10 challenge repeated an hour after the first. If the enhanced effect had been abolished in the second challenge, it may have indicated that receptor desensitization drives the initial robust effect. Instead, the facilitation of the LH response in the second trial may represent changes in Kiss1R in GnRH neurons, changes in downstream receptor signaling/peptide release, or enhanced facilitation of GnRHR in the pituitary. Future studies are needed to determine the exact mechanism of increased kisspeptin responsiveness in the *Bmal1* KO mice.

We found no evidence of disrupted fertility in the Kiss1-Bmal1$^{-/-}$ and GnRH-Bmal1$^{-/-}$ females. In Kiss1 neurons, cell-autonomous circadian rhythms have been described [7]. However, we find no impairment in fecundity or the generation of the LH surge of these mice. In GnRH neurons, endogenous clocks have been described *in vivo* and shown to be important for GnRH release *in vitro* [46]. The Kiss-Cre line expresses Cre in "virtually all" Kiss1 neurons [24] and has been used to produce Kiss1 neuron-specific deletions by a number of groups [47], and the Bmal1$^{fl/fl}$ mouse has been shown to ablate Bmal1 function following Cre exposure in a variety of tissues [16, 19, 48]. Owing to the absence of a well-validated, commercially available Kiss1 antibody, we could not directly measure the efficiency of KO in positively identified Kiss1 neurons; however, we showed Bmal1 recombination in micropunches from the AVPV and ARC but not elsewhere in the brain. Therefore, it is possible that inefficient Bmal1 recombination in Kiss1 neurons is enough to maintain circadian regulation in these neurons. The GnRH-Cre line used has been validated by multiple groups [49, 50], and Cre is detected in ~85% of GnRH neurons [23]. We found no GnRH and Bmal1 colocalization in three of the four GnRH-Bmal1$^{-/-}$ mice we measured, although one mouse did show Bmal1-containing neurons. These may represent the ~15% of GnRH neurons that do not express Cre in this line. Based on our findings of increased AVPV Kiss1 mRNA prior to the time of the surge in the whole-body KO, we would expect that the LH surge is blocked in the *Bmal1* KO by abnormal circadian gating at the level of GnRH neurons; however, we find that these animals are fertile and able to produce an LH surge at the correct time

Gonadotrope-specific *Bmal1* KOs and theca cell–specific *Bmal1* KOs display abnormal estrous cycling in light/dark conditions [16, 51], but it is possible that the use of light/dark conditions may mask a fertility phenotype in the Kiss1-Bmal1$^{-/-}$ and GnRH-Bmal1$^{-/-}$ mice. We addressed this possibility by examining ovarian histology. Because mice can entrain to daily vaginal smears, we used ovarian histology after 6 weeks of constant darkness to determine whether the mice were still showing signs of ovulation, as measured by corpora lutea and Graafian follicles. We found no evidence of disruption through these markers. The increase in Graafian follicles in constant darkness has previously been reported in gerbils [52]. Because this cohort of mice was housed in a separate facility under different conditions, it is entirely possible that this effect is technical rather than biological. Although it is possible that we may have missed more subtle effects that could be detected by daily vaginal cytology, these findings reiterate the absence of a gross reproductive phenotype in these conditional KOs. One possibility for our findings is that the functional SCN provides all of the temporal signaling necessary to drive the LH surge in the Kiss1-Bmal1$^{-/-}$

and GnRH-Bmal1$^{-/-}$ mice. Certainly, the necessity of the SCN in the generation of the LH surge has been repeatedly demonstrated, but these findings may hint that rhythms in the SCN alone are sufficient to drive the surge. Another possibility is that a Bmal1-independent oscillator is sufficient to drive the surge. Ultradian GnRH expression, for instance, is thought to be regulated independently of the canonical circadian clock [45]. Alternatively, it is possible that the "negative arm" of the circadian clock instead regulates the circadian aspect independently of Bmal1, such as Per2 activation by estrogens [53]. Another possibility is that, although the Cre mice used are known to target the vast majority of the respective populations, residual *Bmal1* function in remaining neurons is sufficient to time the preovulatory LH surge.

Overall, our findings begin to decouple the contribution of extra-SCN molecular clocks to the generation of the preovulatory LH surge and fertility. Conditional KO of *Bmal1* in either GnRH or Kiss1 neurons using Cre-Lox technology is insufficient to disrupt the LH surge and fertility, suggesting a role of direct SCN projections to these populations to drive fertility. However, it remains unclear whether the absence of a detectable LH surge in the *Bmal1* KO arises because of altered neural circuitry or a truly canonical circadian effect.

Acknowledgments

We thank Jason D. Meadows, Ichiko Saotome, and Thijs Walbeek for technical assistance on this project, as well as Dan D. Clark for preliminary studies of the GnRH-Bmal1$^{-/-}$ mice. We also thank the staff of the Nikon Imaging Center at the University of California San Diego for microscopy training.

Financial Support: This work was supported by National Institutes of Health Grants R01 HD082567 and R01 HD072754 (to P.L.M.) and by National Institute of Child Health and Human Development/National Institutes of Health Grant P50 HD012303 as part of the National Centers for Translational Research in Reproduction and Infertility (to P.L.M.). P.L.M. was partially supported by National Institute of Diabetes and Digestive and Kidney Diseases Grant P30 DK063491, National Institute of Environmental Health Sciences Grant P42 ES101337, and National Cancer Institute Grant P30 CA023100. Eunice Kennedy Shriver National Institute of Child Health and Human Development Grant T32 HD007203 partially supported K.J.T. and E.L.S. K.J.T. was also partially supported by Eunice Kennedy Shriver National Institute of Child Health and Human Development Grant F32 HD090837. E.L.S. was also partially supported by the Lalor Foundation, National Institute of Environmental Health Sciences Grant P42 ES101337, and by National Institute of Diabetes and Digestive and Kidney Diseases Grant T32 DK007044. L.E.B was partially supported a Dr. Doris A. Howell Foundation undergraduate research scholarship, and L.J.C. was partially supported by the University of California San Diego Frontiers of Innovation Scholars Program, the Endocrine Society Summer Research Fellowship Award, and the Ledell Family Foundation Endowed Research Scholarship for Science and Engineering.

Correspondence: Pamela L. Mellon, PhD, University of California San Diego, 9500 Gilman Drive, La Jolla, California 92093. E-mail: pmellon@ucsd.edu.

Disclosure Summary: The authors have nothing to disclose.

References and Notes

1. Cahill DJ, Wardle PG, Harlow CR, Hull MG. Onset of the preovulatory luteinizing hormone surge: diurnal timing and critical follicular prerequisites. *Fertil Steril.* 1998;**70**(1):56–59.
2. Bunger MK, Wilsbacher LD, Moran SM, Clendenin C, Radcliffe LA, Hogenesch JB, Simon MC, Takahashi JS, Bradfield CA. *Mop3* is an essential component of the master circadian pacemaker in mammals. *Cell*. 2000;**103**(7):1009–1017.
3. Williams WP III, Jarjisian SG, Mikkelsen JD, Kriegsfeld LJ. Circadian control of kisspeptin and a gated GnRH response mediate the preovulatory luteinizing hormone surge. *Endocrinology*. 2011;**152**(2):595–606.
4. Vida B, Deli L, Hrabovszky E, Kalamatianos T, Caraty A, Coen CW, Liposits Z, Kalló I. Evidence for suprachiasmatic vasopressin neurones innervating kisspeptin neurones in the rostral periventricular area of the mouse brain: regulation by oestrogen. *J Neuroendocrinol.* 2010;**22**(9):1032–1039.
5. Horvath TL, Cela V, van der Beek EM. Gender-specific apposition between vasoactive intestinal peptide-containing axons and gonadotrophin-releasing hormone-producing neurons in the rat. *Brain Res*. 1998;**795**(1–2):277–281.

6. Van der Beek EM, Horvath TL, Wiegant VM, Van den Hurk R, Buijs RM. Evidence for a direct neuronal pathway from the suprachiasmatic nucleus to the gonadotropin-releasing hormone system: combined tracing and light and electron microscopic immunocytochemical studies. *J Comp Neurol*. 1997;**384**(4): 569–579.
7. Chassard D, Bur I, Poirel VJ, Mendoza J, Simonneaux V. Evidence for a putative circadian Kiss-clock in the hypothalamic AVPV in female mice. *Endocrinology*. 2015;**156**(8):2999–3011.
8. Hickok JR, Tischkau SA. In vivo circadian rhythms in gonadotropin-releasing hormone neurons. *Neuroendocrinology*. 2010;**91**(1):110–120.
9. Yoo SH, Yamazaki S, Lowrey PL, Shimomura K, Ko CH, Buhr ED, Siepka SM, Hong HK, Oh WJ, Yoo OJ, Menaker M, Takahashi JS. PERIOD2:LUCIFERASE real-time reporting of circadian dynamics reveals persistent circadian oscillations in mouse peripheral tissues. *Proc Natl Acad Sci USA*. 2004; **101**(15):5339–5346.
10. Chappell PE, Goodall CP, Tonsfeldt KJ, White RS, Bredeweg E, Latham KL. Modulation of gonadotrophin-releasing hormone secretion by an endogenous circadian clock. *J Neuroendocrinol*. 2009;**21**(4):339–345.
11. Tonsfeldt KJ, Goodall CP, Latham KL, Chappell PE. Oestrogen induces rhythmic expression of the Kisspeptin-1 receptor GPR54 in hypothalamic gonadotrophin-releasing hormone-secreting GT1-7 cells. *J Neuroendocrinol*. 2011;**23**(9):823–830.
12. Smarr BL, Morris E, de la Iglesia HO. The dorsomedial suprachiasmatic nucleus times circadian expression of *Kiss1* and the luteinizing hormone surge. *Endocrinology*. 2012;**153**(6):2839–2850.
13. Robertson JL, Clifton DK, de la Iglesia HO, Steiner RA, Kauffman AS. Circadian regulation of *Kiss1* neurons: implications for timing the preovulatory gonadotropin-releasing hormone/luteinizing hormone surge. *Endocrinology*. 2009;**150**(8):3664–3671.
14. Ratajczak CK, Boehle KL, Muglia LJ. Impaired steroidogenesis and implantation failure in *Bmal1*$^{-/-}$ mice. *Endocrinology*. 2009;**150**(4):1879–1885.
15. Liu Y, Johnson BP, Shen AL, Wallisser JA, Krentz KJ, Moran SM, Sullivan R, Glover E, Parlow AF, Drinkwater NR, Schuler LA, Bradfield CA. Loss of BMAL1 in ovarian steroidogenic cells results in implantation failure in female mice. *Proc Natl Acad Sci USA*. 2014;**111**(39):14295–14300.
16. Chu A, Zhu L, Blum ID, Mai O, Leliavski A, Fahrenkrug J, Oster H, Boehm U, Storch KF. Global but not gonadotrope-specific disruption of *Bmal1* abolishes the luteinizing hormone surge without affecting ovulation. *Endocrinology*. 2013;**154**(8):2924–2935.
17. Miller BH, Olson SL, Turek FW, Levine JE, Horton TH, Takahashi JS. Circadian clock mutation disrupts estrous cyclicity and maintenance of pregnancy. *Curr Biol*. 2004;**14**(15):1367–1373.
18. RRID:IMSR_JAX:007668, https://scicrunch.org/resolver/IMSR_JAX:007668.
19. Storch KF, Paz C, Signorovitch J, Raviola E, Pawlyk B, Li T, Weitz CJ. Intrinsic circadian clock of the mammalian retina: importance for retinal processing of visual information. *Cell*. 2007;**130**(4):730–741.
20. RRID:IMSR_JAX:003377, https://scicrunch.org/resolver/IMSR_JAX:003377.
21. Schoeller EL, Clark DD, Dey S, Cao NV, Semaan SJ, Chao LW, Kauffman AS, Stowers L, Mellon PL. Bmal1 is required for normal reproductive behaviors in male mice. *Endocrinology*. 2016;**157**(12): 4914–4929.
22. RRID:MGI_4442244, https://scicrunch.org/resolver/MGI_4442244.
23. Wolfe A, Divall S, Singh SP, Nikrodhanond AA, Baria AT, Le WW, Hoffman GE, Radovick S. Temporal and spatial regulation of CRE recombinase expression in gonadotrophin-releasing hormone neurones in the mouse. *J Neuroendocrinol*. 2008;**20**(7):909–916.
24. Cravo RM, Margatho LO, Osborne-Lawrence S, Donato J Jr, Atkin S, Bookout AL, Rovinsky S, Frazão R, Lee CE, Gautron L, Zigman JM, Elias CF. Characterization of *Kiss1* neurons using transgenic mouse models. *Neuroscience*. 2011;**173**:37–56.
25. RRID:IMSR_JAX:023426, https://scicrunch.org/resolver/IMSR_JAX:023426.
26. Postic C, Shiota M, Niswender KD, Jetton TL, Chen Y, Moates JM, Shelton KD, Lindner J, Cherrington AD, Magnuson MA. Dual roles for glucokinase in glucose homeostasis as determined by liver and pancreatic beta cell-specific gene knock-outs using Cre recombinase. *J Biol Chem*. 1999;**274**(1): 305–315.
27. RRID:IMSR_JAX:018961, https://scicrunch.org/resolver/IMSR_JAX:018961.
28. Byers SL, Wiles MV, Dunn SL, Taft RA. Mouse estrous cycle identification tool and images. *PLoS One*. 2012;**7**(4):e35538.
29. Caligioni CS. Assessing reproductive status/stages in mice. *Curr Protoc Neurosci*. 2009;Appendix 4–Appendix 4I.
30. Colledge WH, Mei H, d'Anglemont de Tassigny X. Mouse models to study the central regulation of puberty. *Mol Cell Endocrinol*. 2010;**324**(1–2):12–20.

31. Bosch MA, Tonsfeldt KJ, Rønnekleiv OK. mRNA expression of ion channels in GnRH neurons: subtype-specific regulation by 17β-estradiol. *Mol Cell Endocrinol*. 2013;**367**(1–2):85–97.
32. Franklin KBJ, Paxinos G. *The Mouse Brain in Stereotaxic Coordinates*. San Diego, CA: Academic Press; 1997.
33. RRID:AB_1586907, https://scicrunch.org/resolver/AB_1586907.
34. RRID:AB_2565079, https://scicrunch.org/resolver/AB_2565079.
35. RRID:AB_572248, https://scicrunch.org/resolver/AB_572248.
36. RRID:AB_2336132, https://scicrunch.org/resolver/AB_2336132.
37. RRID:AB_2534079, https://scicrunch.org/resolver/AB_2534079.
38. Schindelin J, Arganda-Carreras I, Frise E, Kaynig V, Longair M, Pietzsch T, Preibisch S, Rueden C, Saalfeld S, Schmid B, Tinevez JY, White DJ, Hartenstein V, Eliceiri K, Tomancak P, Cardona A. Fiji: an open-source platform for biological-image analysis. *Nat Methods*. 2012;**9**(7):676–682.
39. Burel JM, Besson S, Blackburn C, Carroll M, Ferguson RK, Flynn H, Gillen K, Leigh R, Li S, Lindner D, Linkert M, Moore WJ, Ramalingam B, Rozbicki E, Tarkowska A, Walczysko P, Allan C, Moore J, Swedlow JR. Publishing and sharing multi-dimensional image data with OMERO. *Mamm Genome*. 2015;**26**(9–10):441–447.
40. Johnson BP, Walisser JA, Liu Y, Shen AL, McDearmon EL, Moran SM, McIntosh BE, Vollrath AL, Schook AC, Takahashi JS, Bradfield CA. Hepatocyte circadian clock controls acetaminophen bioactivation through NADPH-cytochrome P450 oxidoreductase. *Proc Natl Acad Sci USA*. 2014;**111**(52):18757–18762.
41. Zhang D, Tong X, Arthurs B, Guha A, Rui L, Kamath A, Inoki K, Yin L. Liver clock protein BMAL1 promotes de novo lipogenesis through insulin-mTORC2-AKT signaling. *J Biol Chem*. 2014;**289**(37):25925–25935.
42. DeBruyne JP, Weaver DR, Dallmann R. The hepatic circadian clock modulates xenobiotic metabolism in mice. *J Biol Rhythms*. 2014;**29**(4):277–287.
43. Navarro VM, Castellano JM, Fernández-Fernández R, Tovar S, Roa J, Mayen A, Nogueiras R, Vazquez MJ, Barreiro ML, Magni P, Aguilar E, Dieguez C, Pinilla L, Tena-Sempere M. Characterization of the potent luteinizing hormone-releasing activity of KiSS-1 peptide, the natural ligand of GPR54. *Endocrinology*. 2005;**146**(1):156–163.
44. Gottsch ML, Cunningham MJ, Smith JT, Popa SM, Acohido BV, Crowley WF, Seminara S, Clifton DK, Steiner RA. A role for kisspeptins in the regulation of gonadotropin secretion in the mouse. *Endocrinology*. 2004;**145**(9):4073–4077.
45. Choe HK, Kim HD, Park SH, Lee HW, Park JY, Seong JY, Lightman SL, Son GH, Kim K. Synchronous activation of gonadotropin-releasing hormone gene transcription and secretion by pulsatile kisspeptin stimulation. *Proc Natl Acad Sci USA*. 2013;**110**(14):5677–5682.
46. Chappell PE, White RS, Mellon PL. Circadian gene expression regulates pulsatile gonadotropin-releasing hormone (GnRH) secretory patterns in the hypothalamic GnRH-secreting GT1-7 cell line. *J Neurosci*. 2003;**23**(35):11202–11213.
47. Stephens SB, Tolson KP, Rouse ML Jr, Poling MC, Hashimoto-Partyka MK, Mellon PL, Kauffman AS. Absent progesterone signaling in kisspeptin neurons disrupts the LH surge and impairs fertility in female mice. *Endocrinology*. 2015;**156**(9):3091–3097.
48. Mereness AL, Murphy ZC, Forrestel AC, Butler S, Ko C, Richards JS, Sellix MT. Conditional deletion of *Bmal1* in ovarian theca cells disrupts ovulation in female mice. *Endocrinology*. 2016;**157**(2):913–927.
49. Novaira HJ, Sonko ML, Hoffman G, Koo Y, Ko C, Wolfe A, Radovick S. Disrupted kisspeptin signaling in GnRH neurons leads to hypogonadotrophic hypogonadism. *Mol Endocrinol*. 2014;**28**(2):225–238.
50. Diaczok D, DiVall S, Matsuo I, Wondisford FE, Wolfe AM, Radovick S. Deletion of *Otx2* in GnRH neurons results in a mouse model of hypogonadotropic hypogonadism. *Mol Endocrinol*. 2011;**25**(5):833–846.
51. Mereness AL, Murphy ZC, Sellix MT. Developmental programming by androgen affects the circadian timing system in female mice. *Biol Reprod*. 2015;**92**(4):88.
52. Sinhasane SV, Joshi BN. Melatonin and exposure to constant light/darkness affects ovarian follicular kinetics and estrous cycle in Indian desert gerbil *Meriones hurrianae* (Jerdon). *Gen Comp Endocrinol*. 1997;**108**(3):352–357.
53. Gery S, Virk RK, Chumakov K, Yu A, Koeffler HP. The clock gene Per2 links the circadian system to the estrogen receptor. *Oncogene*. 2007;**26**(57):7916–7920.